

Article

# Characteristics of Atmospheric Inorganic Nitrogen Wet Deposition in Coastal Urban Areas of Xiamen, China

Yao Feng <sup>1,2</sup>, Shuhui Zhao <sup>1,2</sup>, Shanshan Wang <sup>1,2</sup>, Qi Lin <sup>1,2</sup>, Yang Luo <sup>1,2</sup>, Suqing Xu <sup>1,2</sup>, Hang Yang <sup>1,2</sup>, Jun Shi <sup>1,2</sup>, Miming Zhang <sup>1,2</sup>, Liping Jiao <sup>1,2</sup> and Jinpei Yan <sup>1,2,\*</sup>

<sup>1</sup> Key Laboratory of Global Change and Marine Atmospheric Chemistry, MNR, Xiamen 361005, China; fengyao@tio.org.cn (Y.F.); shzhao@tio.org.cn (S.Z.); wangshanshan1336@tio.org.cn (S.W.); linqi@tio.org.cn (Q.L.); luoyang@tio.org.cn (Y.L.); xusuqing@tio.org.cn (S.X.); yanghang@tio.org.cn (H.Y.); shijun@tio.org.cn (J.S.); zhangmiming@tio.org.cn (M.Z.); jiaoliping@tio.org.cn (L.J.)  
<sup>2</sup> Third Institute of Oceanography, Ministry of Natural Resources, Xiamen 361005, China  
 \* Correspondence: jpyan@tio.org.cn



**Citation:** Feng, Y.; Zhao, S.; Wang, S.; Lin, Q.; Luo, Y.; Xu, S.; Yang, H.; Shi, J.; Zhang, M.; Jiao, L.; et al. Characteristics of Atmospheric Inorganic Nitrogen Wet Deposition in Coastal Urban Areas of Xiamen, China. *Atmosphere* **2021**, *12*, 1447. <https://doi.org/10.3390/atmos12111447>

Academic Editor: Young-Ji Han

Received: 16 September 2021

Accepted: 27 October 2021

Published: 2 November 2021

**Publisher's Note:** MDPI stays neutral with regard to jurisdictional claims in published maps and institutional affiliations.



**Copyright:** © 2021 by the authors. Licensee MDPI, Basel, Switzerland. This article is an open access article distributed under the terms and conditions of the Creative Commons Attribution (CC BY) license (<https://creativecommons.org/licenses/by/4.0/>).

**Abstract:** To evaluate the impact of increasing atmospheric nitrogen deposition input to the coastal ecosystem, measurements were conducted to analyze the inorganic nitrogen wet deposition to Xiamen Island during April to August in 2014. Using ion chromatography and shown to contain main nine water-soluble ions—including Na<sup>+</sup>, NH<sub>4</sub><sup>+</sup>, K<sup>+</sup>, Mg<sup>2+</sup>, Ca<sup>2+</sup>, Cl<sup>-</sup>, NO<sup>-</sup>, NO<sub>3</sub><sup>-</sup>, and SO<sub>4</sub><sup>2-</sup>—we analyzed the composition of the wet deposition sample and verified the contribution of different ions to the different sources. The results showed that the mean NO<sub>3</sub><sup>-</sup>-N and NH<sub>4</sub><sup>+</sup>-N concentration in rainfall for five months was 4.55 ± 5.15 mg·L<sup>-1</sup> (*n* = 31) and 1.20 ± 1.16 mg·L<sup>-1</sup> (*n* = 33), respectively. Highest NO<sub>3</sub><sup>-</sup>-N (74.65 mg·N·L<sup>-1</sup>) and NH<sub>4</sub><sup>+</sup>-N (16.06 mg·N·L<sup>-1</sup>) values were both observed in May. Maximum NO<sub>3</sub><sup>-</sup>-N deposition (507.5 mg·N·m<sup>-2</sup>) was also in May, while the highest NH<sub>4</sub><sup>+</sup>-N deposition (99.8 mg·N·m<sup>-2</sup>) was in June. The total inorganic wet nitrogen flux during sampling period was 11.1 kg·N·ha<sup>-1</sup>. The HYSPLIT backward air masses trajectory and USEPA PMF model was used, as the composition of the air masses passing over the sample area were impacted from three sources: fertilizers and biomass combustion, formation of secondary aerosol, and Marine aerosols. The concentration ratio of SO<sub>4</sub><sup>2-</sup> and NO<sub>3</sub><sup>-</sup> in ranged between 0.5 and 3 in rainfall samples with an average of 1.34, suggesting that the contribution from vehicle exhaust to air pollution in the sample area is increasing. Long-term continuous monitoring of wet deposition in this region needs to be expanded to fully understand the impacts of human activity on air quality and to quantify N deposition to local marine ecosystems.

**Keywords:** wet deposition; water-soluble ions; inorganic nitrogen deposition fluxes

## 1. Introduction

Nitrogen is an essential biogenic element and is one of the most complex elements with many valence states. Nitrogen is a limiting factor for biological productivity, which gives it a central role in oceanic biogeochemical cycles. The wet deposition of atmospheric nitrogen is the process by which nitrogen is deposited in terrestrial or aquatic ecosystems by raindrops or snowfall. Atmospheric nitrogen deposition in the Taihu Lake area is one of the largest contributors of nitrogen pollution, second only to loss of nitrogen from farmland [1]. Precipitation chemistry and sedimentation rates are important factors for understanding and predicting the impacts of anthropogenic atmospheric discharge on ecosystems [2].

The rapid expansion of the global population has been accompanied by an increase in N emissions and a subsequent increase in N deposition. There has been a non-negligible increase in atmospheric nitrogen deposition year by year due to increases in certain human activities (such as fossil fuel emissions, artificial fertilizers, etc.), and this deposition into the natural environment has put a heavy pressure on ecosystems. Specifically, the growth in number of motor vehicles has led to increased oxynitride emissions since 2000 [3].

It is generally believed that the main sources of  $\text{NH}_4^+$  in aerosol are agricultural activities associated with fertilizer application and livestock production [4]. The application of fertilizers and the release of animal waste leads to increases in  $\text{NH}_3$  emissions. However, the high N concentrations from other sources such as fossil fuel emissions are occurring in certain times of year [5]. Deposited  $\text{NH}_4^+$ -N accounts for 58.7% of all wet deposition, coming primarily in the form of wet deposited dissolved inorganic nitrogen (DIN) at road monitoring stations in the United States [6]. Studies of nitrogen deposition around Boston, USA showed that rates in cities were about twice as high as those in nearby rural areas [7]. Urban sites have different N sources than rural areas and population centers in mountainous areas. In addition, precipitated DIN has the potential to negatively impact both aquatic and terrestrial ecosystems [8].

Due to the increasing trend in the magnitude of N deposition, many recent studies have been focused on the effects of N-loading on forests, basins, deltas, and other inland areas. However, there have been relatively few studies on N deposition in the open sea and coastal areas. The dry deposition of N in the Huang-Huai-Hai Plain contributed the majority of the total N deposition, with an average contribution of 65%. Seasonal differences, active nitrogen source species, site management, underlying surfaces, vegetation conditions, and weather conditions will all affect atmospheric nitrogen deposition and its composition [9]. Rural dry deposition in the Beijing area accounted for 75% of all nitrogen deposition, while wet deposition accounted for 25% [10]. Similarly, total inorganic nitrogen deposition in the Pearl River Delta and Guangdong Province was dominated by dry deposition, which accounted for 63.8% and 61.1%, respectively. Generally,  $\text{NH}_4^+$  is the main component of wet deposition, while  $\text{NH}_3$ -N is the main component of dry deposition [11]. While the chemistry of wet deposition is generally well characterized at individual sampling locations for short periods of time, there remains large uncertainty in the overall spatial variability of N deposition across China. This is due in part to the lack of a nationwide continuous deposition monitoring network. In order to better evaluate the impact of nitrogen deposition, it is necessary to monitor the wet and dry nitrogen deposition across the country. The anthropogenic application of nitrogen fertilizers in the central subtropical agricultural basin have resulted in significant  $\text{NH}_3$  emissions. It is essential to reduce anthropogenic N emitting activities (nitrogen fertilization, animal production, and fossil fuel combustion) in this subtropical region to prevent irreversible damage to its fragile ecosystems [12]. The national average nitrogen deposition rates have varied greatly from year to year, in some cases by as much as 59%. In addition, the data have shown that nitrogen deposition rates have been increasing in hotspots in the southeastern portion of China [13].

Xiamen's air quality ranked second among cities that are prefecture-level and above in China all year round. A small increase in  $\text{PM}_{2.5}$  particles, like those from vehicle exhaust, will have a significant impact on air quality. According to the Yearbook of Xiamen Special Economic Zone of 2014 (<http://www.xm.gov.cn/zwgk/tqjj/xmjttqnj/>, accessed on 10 September 2021), the number of tourist and civilian vehicles in Xiamen reached 632.7 million and 1.2 million, respectively, which coincided with the increased population density of Xiamen Island. Human influence through the use of waste treatment systems (e.g., septic tanks, sewage treatment plants, and landfills) and various modes of transportation accounted for up to 92.4% of the total  $\text{NH}_3$  emitted within the Siming District of Xiamen Island in 2015 [14]. Stable isotope mixing models have shown that fossil fuel-related  $\text{NH}_3$  emissions (fossil fuel combustion) contributed more than 70% of the aerosol  $\text{NH}_4^+$  [15].

Using the MFA (material flow analysis) method to create a detailed model of nitrogen flow, the results showed that increasing the removal rate of  $\text{NO}_x$  emissions at the point of fossil fuel consumption and adopting management practices within the surrounding watersheds to limit the loss of N-containing compounds would greatly help reduce the presence of N-containing pollutants in the Xiamen region [16]. Without substantial control of  $\text{NH}_3$  emissions, model simulations indicate that effective reduction in formation of aerosols in the  $\text{PM}_{2.5}$

fraction will be limited if emphasis is solely on reducing SO<sub>2</sub> and NO<sub>x</sub> emissions [17–19]. Reducing nitrogen emissions to the environment should be prioritized moving forward.

Recently, research in the Xiamen area has been focused on the deposition and characterization of the PM<sub>2.5</sub> and PM<sub>10</sub> fractions in the atmosphere, including the presence of various trace metals, salt-forming ions, organic and elemental carbon content, and other substances [20–22]. While the PM fraction is an important component of air quality, it is not the only source of N-deposition. The continuous and long-term collection of wet deposition needs to continue and be strengthened throughout the area to fully understand N inputs. In this paper, we focus on wet deposition during a single rainy season in the Xiamen region and characterize the chemistry and magnitude of nitrogen inputs. The rainy season accounts for ~70% of the total precipitation received and a substantial amount of the N-loading to this coastal urban area. The source of aerosols captured by wet deposition were analyzed using the USEPA PMF (positive matrix factorization) model to better understand the variability in nitrogen wet deposition amounts associated with individual rain events. These results illustrate the importance of monitoring wet deposition to help understand the impacts of atmospheric nitrogen on marine nutrient cycling in coastal areas.

## 2. Methods and Materials

### 2.1. Sampling Site

The sample site was located in the southwest portion of Xiamen Island near the city of Xiamen (latitude and longitude information here). Xiamen is an important central city along the southeast coast of China. The sampling equipment was mounted on a wooden platform located on the roof of the research building for the Third Institute of Oceanography at an altitude of 45 m. The sampling equipment is designated as the regional background station of the marine atmospheric environment monitoring system, and is considered representative of an urban coastal area in China. Nearby urban influences include Xiamen University, Gulangyu Island, and Nanputuo Temple as well as other scenic locations frequented by visitors throughout the year (Figure 1). Urban emissions include activities from a nearby harbor. It is affected by residential, oceans, and ships emission. The selected place is relatively representative.

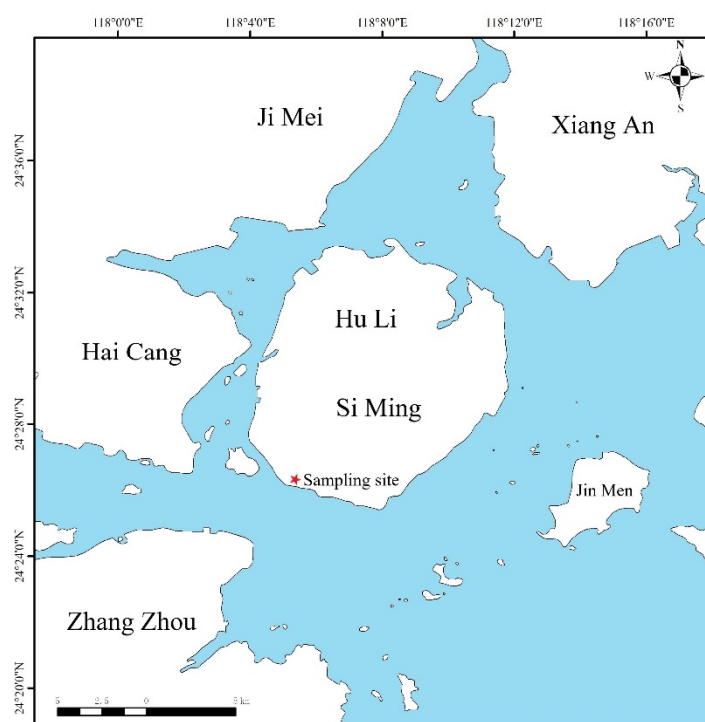
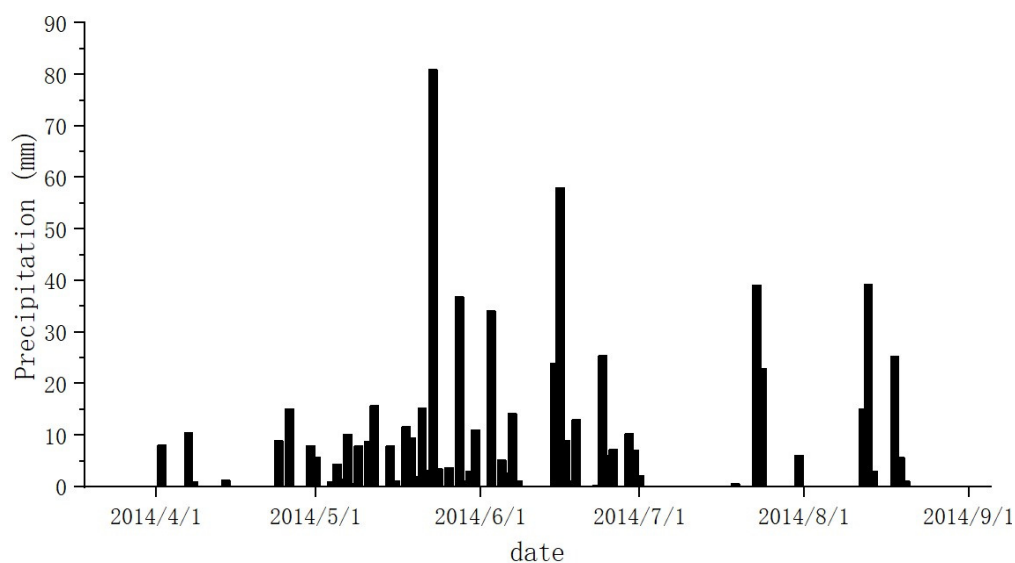


Figure 1. Map of the sampling site.

## 2.2. Precipitation

Xiamen Island is located in a subtropical monsoon climate within a subtropical high-pressure zone. The spring and summer periods are from March to May and April to June, respectively. Wet deposition samples were collected from the beginning of 2014 to the end of August that year, for a total of 42 individual samples. To the extent possible, each sample collected represented a single rainfall event. Of this number, samples were excluded if the concentration of the chemical species of interest were below analytical detection limits. Using these criteria, only events from April to August 2014 were used in this study. This included the bulk of the 2014 rainy season at this location. The precipitation in 2014 was close to that of previous years in Xiamen, mainly concentrated in the rainy season (April to June) during spring and summer as shown in Figure 2. Heavy precipitation events occurred in May, July, and August. The total annual precipitation in 2014 was 1084.5 mm, and the total precipitation during the sampling period was 675.4 mm, or about 62% of the annual precipitation. The precipitation during different months varied as follows: 52.38 mm in April, 245.61 mm in May, 217.76 mm in June, 70.54 mm in July, and 89.09 mm in August. During the sampling period, the daily precipitation ranged from 0.1 mm to a maximum of 80.9 mm. The maximum (80.9 mm) occurred on 23 May 2014 due to the heavy rains driven by the southwest low-level jet stream, which provides a large amount of moisture and unstable energy [23]. Typhoon Hagibis on 16 June 2014 and Typhoon Matmo on 23 July 2014 also brought strong single-day precipitation events to Xiamen, coinciding with the values of 57.91 mm and 39.12 mm, respectively. In 2014, 55.84% of the annual precipitation occurred from April to June, which exceeded the normal total rainfall for this period.



**Figure 2.** The precipitation events during the sampling period.

## 2.3. Sample Apparatus and Methods

An automatic precipitation and dust sampler (TE-78-100XAPS, TISCH, New York, NY, USA) was used to collect precipitation samples from April to August 2014. The sampler was composed of a rain sensor, a wet container, a dry container, and a dust cover. When rain falls, a sensor triggers the cover to move over the dry container and expose the wet container to the rain. When the heated sensor dries, the cover returns to the wet container (typically in about 15 to 20 min) to prevent dust from entering, while at the same time uncovering the dry deposition sampling container. All unfiltered samples were transferred to the pre-cleaned polyethylene plastic bottles with screw top lids and then stored at  $-18^{\circ}\text{C}$  to prevent stabilize the collected samples. All plastic buckets and polyethylene plastic bottles were washed with deionized water at least three times before and after use, and then airdried in a clean room.

For chemical analysis, the thawed rainwater samples were used to rinse out the autosampler vials three times before filling each vial with sample. The autosampler vials were then capped and placed in an appropriate analysis tray. The whole process of analysis and testing was conducted at room temperature (25 °C) and at a humidity less than 80%. All samples were analyzed by DIONEX ICS-2500 and DIONEX ICS-90A ion chromatographs for soluble inorganic ions. The MDL (minimum detection limits) of Na<sup>+</sup>, NH<sub>4</sub><sup>+</sup>, K<sup>+</sup>, Mg<sup>2+</sup>, Ca<sup>2+</sup>, Cl<sup>-</sup>, NO<sup>-</sup>, NO<sub>3</sub><sup>-</sup>, SO<sub>4</sub><sup>2-</sup> were 0.02, 0.009, 0.02, 0.02, 0.05, 0.003, 0.02, 0.03, and 0.004 mg/L, respectively.

Deposition of the individual ionic species for the sampling season was calculated using Equation (1)

$$F_n = \sum_{i=1}^n C_i * P_i \quad (1)$$

where,  $F_n$  is the ion flux;  $n$  is the number of samples;  $C_i$  is the concentration of ion in individual precipitation sample; and  $P_i$  is the individual amount of rainfall during the experiment.

#### 2.4. Data Processing

##### 2.4.1. PMF (Positive Matrix Factorization) Source Resolution Method

This paper used the positive matrix factorization (PMF5.0) (<https://www.epa.gov/air-research/positive-matrix-factorization-model-environmental-data-analyses>, accessed on 10 September 2021) developed by EPA (US Environmental Protection Agency) and principal component analysis (PCA) to conduct the source analysis. PMF5.0 does not require the measurement of the source component spectrum, but analyzes the source spectrum and contribution rate of all kinds of sources using constrained conditions, which also ensures that the elements in the decomposition matrix are non-negative [24].

Use of the PMF5.0 model requires an uncertainty analysis for each chemical species of interest. Estimates of the uncertainty (Unc) were obtained using either Equation (2) or (3).

$$\text{Unc} = \frac{5}{6} * \text{MDL} \quad (2)$$

$$\text{Unc} = \sqrt{\text{ErrorFraction} \times \text{concentration} + (0.5 \times \text{MDL})} \quad (3)$$

If the measured concentration was <MDL, then Equation (2) was used to calculate Unc. If the concentration was >MDL, the Error Fraction term in Equation (3) was assigned a value of 0.1, or 0.2 for species in the PM<sub>2.5</sub> fraction.

##### 2.4.2. Air Mass Trajectory Analysis (HYSPLIT)

Developed by the National Oceanic and Atmospheric Administration (NOAA) Air Resources Laboratory (ARL; <http://www.arl.noaa.gov/ready/hysplit4.html>, accessed on 10 September 2021), the HYSPLIT model trajectories were based on Global Data Assimilation System (GDAS) meteorological data, gridded at a 1° spatial resolution. This was used to investigate the origins of the aerosols and the influence of regional transport on air pollution at the sampling site by analyzing the backward trajectories of air masses [25].

### 3. Results and Discussion

#### 3.1. Characteristics, Concentrations, and Monthly Variations of Water-Soluble Ions

SO<sub>4</sub><sup>2-</sup>, NO<sub>3</sub><sup>-</sup>, Cl<sup>-</sup>, and NH<sub>4</sub><sup>+</sup> were the main water-soluble ions, they accounted for 36.04%, 29.91%, 10.80%, and 8.67% of the total ion mass of the samples, respectively. Seasonal variability of both cations and anions are shown in Figure 3. The sum of the mass of these four ions accounted for 85.4% of the total mass of water-soluble ions, suggesting that secondary aerosols were the dominant source of these ions in the samples. Analysis of separate PM<sub>2.5</sub> fractions indicated that SO<sub>4</sub><sup>2-</sup>, NO<sub>3</sub><sup>-</sup>, and NH<sub>4</sub><sup>+</sup> accounted for more than 80% of the mass present [15].

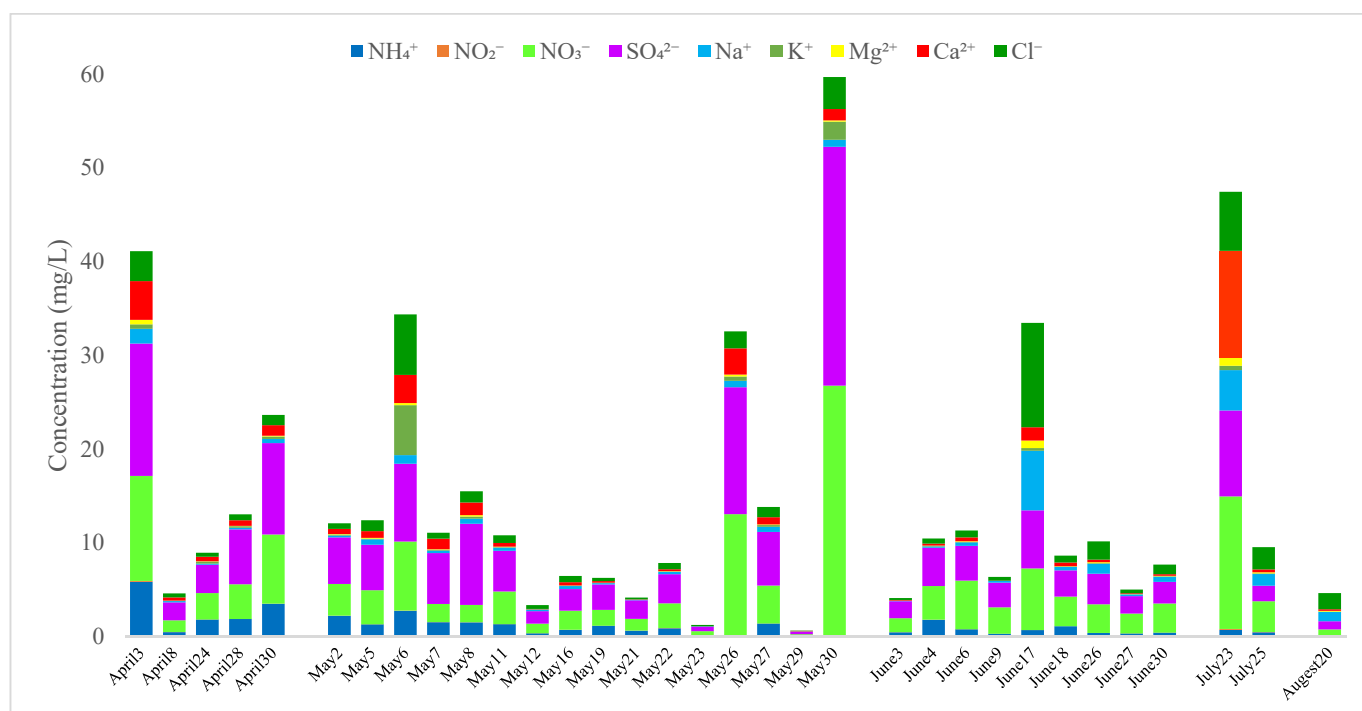


Figure 3. The water-soluble ions in sample.

High values of nitrate and ammonium appeared in spring with relatively lower values in summer (Figure 3). These findings were the same as those PM<sub>2.5</sub> samples in 2016 in Xiamen, with both ions showing higher concentrations in winter and spring than summer and fall [26].

### 3.2. Sources of Fine Particles Using PMF

According to PCA and PMF analysis methods, it can be assumed that the nine water-soluble inorganic ions in the wet deposition samples of Xiamen in spring and summer of 2014 came from three sources, as shown in Figure 4a–c, respectively.

As we can see from the PCA, the left y-axis represents the mass fraction of each species, the right y-axis represents the percentage of each ion's contribution to a certain factor. (Principal component) PC1 represented the contributions of K<sup>+</sup>, NH<sub>4</sub><sup>+</sup>, and Ca<sup>2+</sup>, so it was identified as artificial fertilization and also biomass combustion. Indeed, biomass burning in Beijing has been shown to be a regular pollution factor that cannot be ignored [27]. PC2 reflected the formation of secondary aerosols caused by the burning of fossil fuels and automobile exhaust emissions, which contain high levels of sulfates and nitrates, just as previously discussed. These high concentrations of sulfates and nitrates serve as precursors for PM<sub>2.5</sub> particulate formation. PC3 was closely related to sea salt aerosols due to its high levels of Na<sup>+</sup> and Cl<sup>-</sup>, which are distinctive sea salt ions, as well as the high concentrations of Mg<sup>2+</sup> ions. Sea salt is a large natural source that contributes most of the Cl<sup>-</sup> and Na<sup>+</sup> in aerosols [28]. When clean air masses from the ocean were dominant, the contributions of other ions in the deposition sample were significantly reduced.

The contributions of different factors to the concentrations of the nine kinds of ions are shown in Figure 5. NO<sub>3</sub><sup>-</sup> and SO<sub>4</sub><sup>2-</sup> mainly came from secondary aerosols; the nitrogen and sulfur oxides emitted from industrial activities and automobile exhaust undergo a series of thermochemical and photochemical transformations and become a part of the secondary pollutant aerosols. NH<sub>4</sub><sup>+</sup> and K<sup>+</sup> mainly came from anthropogenic activities such as fertilization and biomass combustion. Ca<sup>2+</sup> mainly came from crustal dust and industrial pollution. Sea salt aerosols usually come from breaking waves and ocean air masses, and include different concentrations of Na<sup>+</sup>, Cl<sup>-</sup>, Mg<sup>2+</sup>, Ca<sup>2+</sup>, SO<sub>4</sub><sup>2-</sup>, etc.

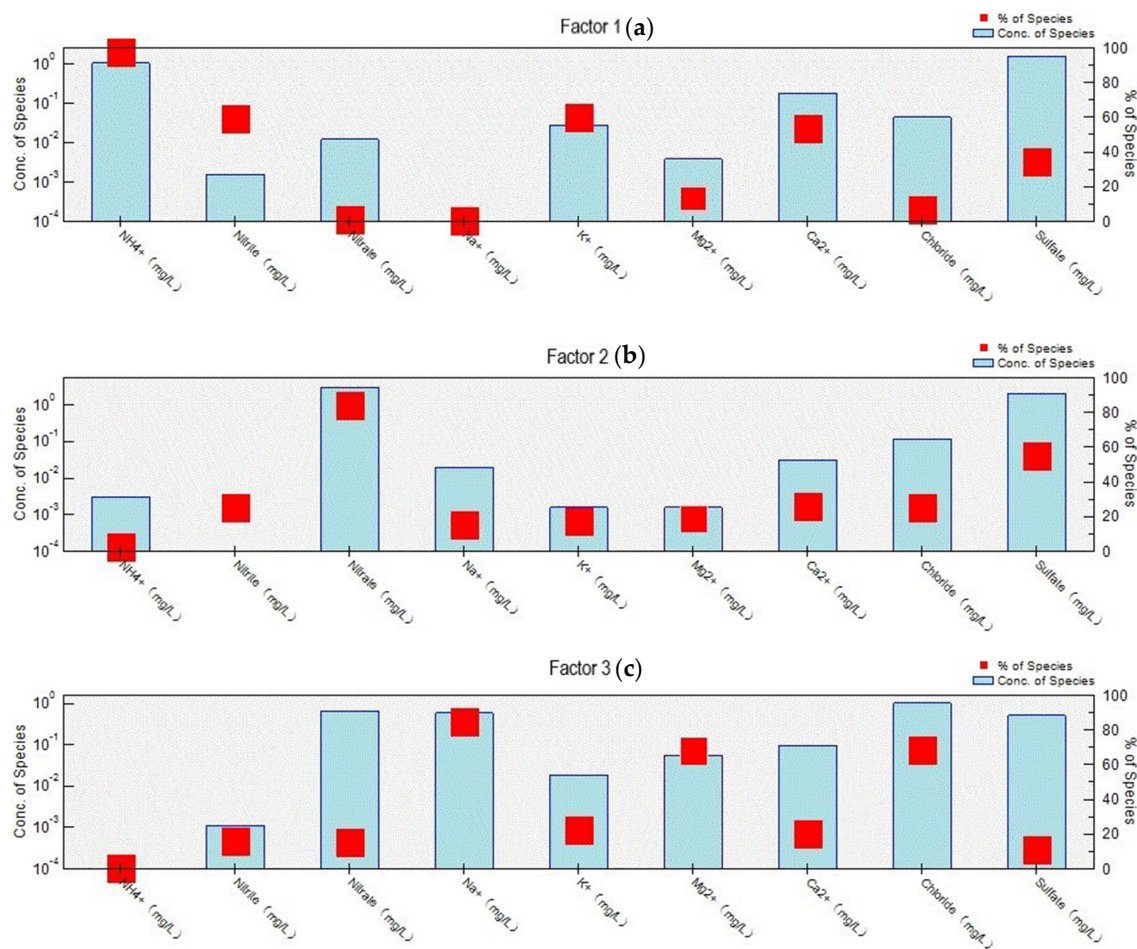


**Figure 4.** The contribution of different factors: (a) Factor 1 represents fertilization and also biomass combustion. Biomass burning; (b) Factor 2 represents secondary aerosols; (c) Factor 3 represents sea salt aerosol of marine source.

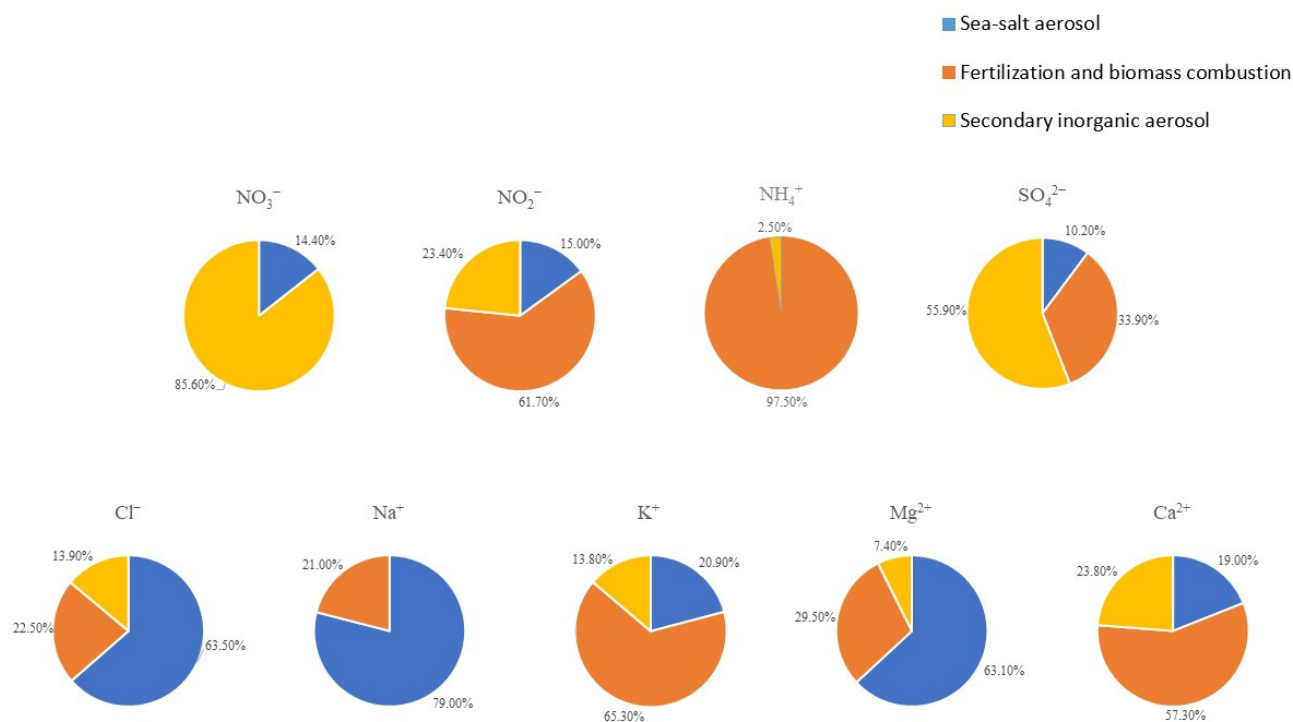


**Figure 5.** Contribution from different factor as a result of PMF modeling.

### 3.3. Nitrogen Wet Deposition

There were four air mass clusters that had an effect on study area during the sampling period (Figure 6). T\_1 represented the air masses that were transported long-distances from the northern continental area, while T\_4 represented the ocean air masses transported over long-distances from the South China Sea. T\_2 and T\_3 represented oceanic air masses from the Northwest Pacific Ocean and South China Sea, respectively. The precipitation in April was mainly affected by air masses from the north. The precipitation in May was mainly affected by the confluence of heating and cooling flows, and the precipitation in summer (June to August) was mainly controlled by oceanic air masses.

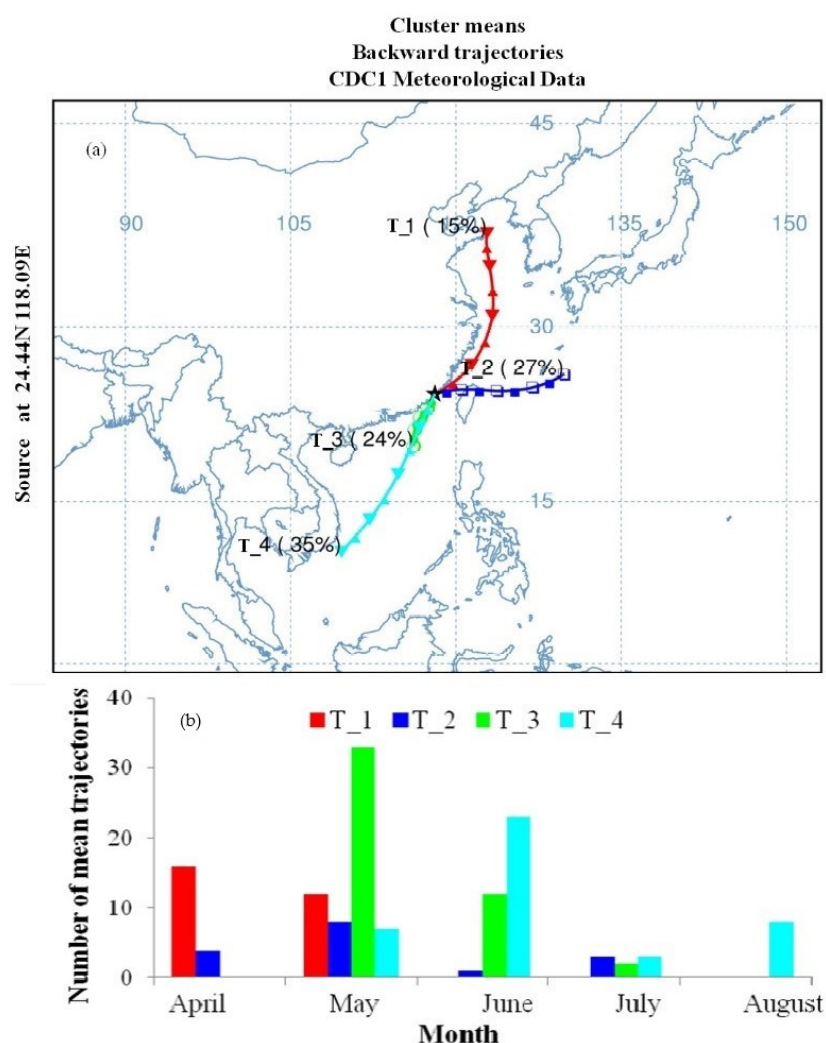


**Figure 6.** (a) Cluster mean trajectories ending site and (b) monthly distributions during sampled precipitation events from April to August [23].

The concentration of  $\text{NO}_3^-$ -N in the sampling site varied from 9.46 mg/L to 74.65 mg/L in different months, and an abnormally high concentration in May (74.65 mg/L) was caused mainly by clusters T\_1 and T\_3 (Figure 7). The secondary pollution aerosols that are not flow out of the city were scoured by the rain, leading to high deposition rates. Generally, the deposited nitrogen came mainly from local motor vehicle exhaust emissions. The monthly variation of  $\text{NH}_4^+$ -N in this region ranged from 1.18 mg/L to 16.06 mg/L. The concentrations of  $\text{NO}_3^-$ -N and  $\text{NH}_4^+$ -N in this region were both high in spring, but low in summer. Their trends of change were the same as those of WIOC (water-insoluble organic carbon) and EC (element carbon) due to the clean air masses from the ocean [23]. In fact, the great variability in sea salt aerosols, especially during the rainy season, was

largely dependent on precipitation due to the wet deposition removal effect [29]. In spring, Xiamen is mainly affected by the northeast monsoon which is influenced by air masses from north China. These air masses typically have high concentrations of potential pollutants. The air masses combine with local air masses that are somewhat stagnant, resulting in relatively higher concentrations of potential pollutants. This results in increased formation of aerosols. In the summer, the southeast monsoon prevails with increased temperatures and rainfall. With the increase in the intensity of rainfall, combined with strong winds, particles in the air are diluted and flushed away, which explains why the concentrations of nitrogen in summer rainwater were generally low. Despite the low concentrations, results have shown that the amount of precipitation is still the main factor affecting nitrogen wet deposition [30].

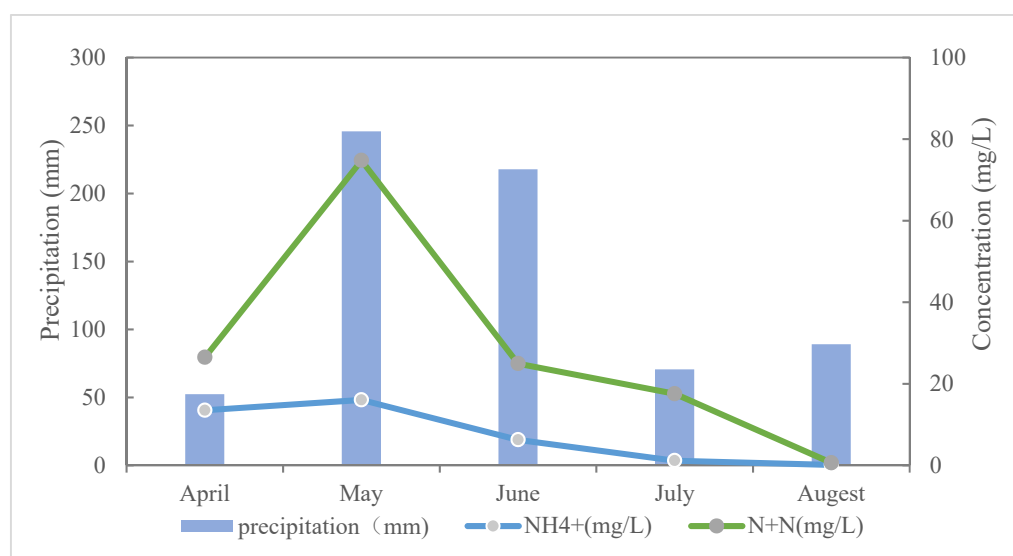


**Figure 7.** Trends of precipitation and ionic inorganic nitrogen.

As we know, the primary ions in precipitation, such as nitrate ions, mainly come from biogenic emissions and automobile exhaust. Sulfate ions are mainly affected by industrial sources and the combustion of various fossil fuels. The ratio of  $\text{SO}_4^{2-}$  to  $\text{NO}_3^-$  is often used as an indicator of the relative contribution of coal burning emission sources and vehicle exhaust emission sources. Compared to previous studies, the  $\text{SO}_4^{2-}$  to  $\text{NO}_3^-$  ratio in summer was higher, suggesting that the particular cause of the high  $\text{SO}_4^{2-}$  values was dominated by coal burning and electric field combustion, while at the same time  $\text{NO}_3^-$  concentrations were reduced through reactions with sea salt ions from the marine air mass to produce coarse-mode  $\text{NaNO}_3$ . In this experiment, the ratio of  $\text{SO}_4^{2-}$  to  $\text{NO}_3^-$  was 1.34 on average, indicating that air pollution caused by vehicle exhaust emissions was increasing, compared with the previous sulfuric acid rain type in China [31]. In summer (June to August) the  $\text{SO}_4^{2-}$  to  $\text{NO}_3^-$  ratio was 0.92, which was also higher than in previous years. This could have been due to reductions in coal burning, improved desulfurization technologies, or an increase in the number of civilian vehicles. Moreover,  $\text{NH}_4^+$  plays an important role in the formation of secondary aerosols, significantly affecting the composition of polluting atmospheric particles in Xiamen [15]. A significant contribution of  $\text{NH}_4^+$  to N deposition was also observed, which indicated that controlling  $\text{NH}_3$  emissions should be prioritized in the future [32].

### 3.4. Wet N Deposition Flux

#### 3.4.1. Calculated Flux Values

The monthly deposition of  $\text{NH}_4^+$  and  $\text{NO}_3^-$  ranged from 3.0 to 99.8  $\text{mg}\cdot\text{N}\cdot\text{m}^{-2}\cdot\text{month}^{-1}$  and 4.6 to 507.5  $\text{mg}\cdot\text{N}\cdot\text{m}^{-2}\cdot\text{month}^{-1}$ , respectively. Wet deposition fluxes of  $\text{NO}_3^- + \text{NO}_2^-$

and  $\text{NH}_4^+$  during this experimental sampling ( $\text{mg}\cdot\text{N}\cdot\text{m}^{-2}\text{month}^{-1}$ ) were as follows in Table 1.

**Table 1.** Monthly water-soluble N wet deposition fluxes.

Month	Wet Deposition			
	$\text{NH}_4^+$	$\text{NO}_3^-$	$\text{NO}_2^-$	N + N
Apr	96.7	54.8	0.3	55.2
May	76.5	507.5	0.9	508.4
Jun	99.8	200.9	0.3	201.2
Jul	22.3	46.0	0.5	46.5
Aug	3.0	4.6	0.1	4.7
Total	298.4	813.9	2.1	815.9
Average	59.7	162.8	0.4	163.2

Unit:  $\text{mg}\cdot\text{N}\cdot\text{m}^{-2}$ . N + N:  $\text{NO}_3^- + \text{NO}_2^-$ .

The highest ammonium nitrogen deposition occurred in June with a value of  $99.8\text{ mg}\cdot\text{N}\cdot\text{m}^{-2}\text{month}^{-1}$ , and another high  $\text{NH}_4^+$  value of  $96.7\text{ mg}\cdot\text{N}\cdot\text{m}^{-2}\text{month}^{-1}$  appeared in April. It was found that the precipitation in April was mainly driven by the air mass transported from the northern continent, which was a different than the source for the high value in June. The wet deposition flux in May was mainly influenced by the confluence of heating and cooling flows, which was caused by the air flow exchange between the northern mainland and the South China Sea. Under the combined influence of high concentrations and precipitation, nitrate nitrogen reached a maximum value of  $507.5\text{ mg}\cdot\text{N}\cdot\text{m}^{-2}\text{month}^{-1}$ , accounting for 62.4% of the total nitrate deposition during the sampling period. The total nitrate nitrogen and ammonium nitrogen depositions were  $8.1\text{ kg}\cdot\text{N}\cdot\text{ha}^{-1}$  and  $2.98\text{ kg}\cdot\text{N}\cdot\text{ha}^{-1}$ , respectively. In the rainy season from April to June, the average fluxes were  $91.0\text{ mg}\cdot\text{N}\cdot\text{m}^{-2}\text{month}^{-1}$  and  $254.4\text{ mg}\cdot\text{N}\cdot\text{m}^{-2}\text{month}^{-1}$ , accounting for 91% and 94% of the total deposition during the sampling period. In the Xiamen region, the amount of atmospheric inorganic nitrogen deposition including dry N deposition accounted for 10.2% of the total nitrogen input in 2018, only after the input of the Jiulong River [33]. The precipitation from June to August was mainly controlled by the long-range transportation of a marine air mass from the South China Sea. Under the abundant precipitation and the centralized scour and obvious removal effect, the overall concentration of nitrogen ions in the atmosphere was reduced and the overall deposition was not high. The high dry  $\text{NO}_3^-$  deposition rate in the East China Sea was related to air masses from northeastern China and central South Korea. In contrast, the wet deposition rates of  $\text{NO}_3^-$  and  $\text{NH}_4^+$  were more or less equal, and the concentrations of these ions may have been related to cloud removal [34]. In order to determine the drivers behind the variability in nitrogen deposition, differences in the factors that influence N deposition were examined in different regions. The results showed that precipitation had the greatest impact on wet deposition in summer when the concentrations of nitrogen gases and particles in the atmosphere were low and precipitation was abundant. However, in spring, when precipitation was low, the concentrations of gaseous and particle ammonia were higher than in other seasons. The high rates of nitrogen deposition in spring and summer reflected the higher precipitation during these seasons.

### 3.4.2. Calculated Flux Values for Coastal Areas of China

Tables 2 and 3 compared our wet N deposition with those reported in the literature for coastal urban areas. In the Pearl River Delta, urban areas have higher nitrogen emission reduction potential than rural areas [30]. The urban N flux was significantly higher than that of town and rural sites, and the wet deposited N had similar N sources in rural and townsites, which was different from that of urban sites [35]. Wet deposition was the main source of atmospheric nitrogen input to the Yellow Sea, accounting for 68% of the total

nitrogen input. Due to the heavy rainfall in summer, the total deposition during this season accounted for 51% of the total deposition over 9 months [36].

The North China region ranged between 16.3 and 28.2 kg·N·ha<sup>-1</sup> a<sup>-1</sup> [37,38], the Yangtze River Delta region was 26.8 kg·N·ha<sup>-1</sup> a<sup>-1</sup> [39], the city of Guangzhou was 27.4 kg·N·ha<sup>-1</sup> a<sup>-1</sup> [40], the Tailake region was 27 kg·N·ha<sup>-1</sup> a<sup>-1</sup> [41], and the Sichuan Basin was 22.5 kg·N·ha<sup>-1</sup> a<sup>-1</sup> [42]. The average value for East Asia was 32.4 kg·N·ha<sup>-1</sup> a<sup>-1</sup> [43], which was similar to many parts of China. The deposition flux of our observed flux that was mainly concentrated on the rainy season data was lower than the other found over many areas of coastal and inland China areas. Compared with 1.7–3.5 kg·N·ha<sup>-1</sup> a<sup>-1</sup> in the United States [44] and 6.58 kg·N·ha<sup>-1</sup> a<sup>-1</sup> in Europe [45], which are the other two N deposition hotspots in the world, more research and emission reductions should be prioritized and implemented (Table 3).

**Table 2.** Wet N deposition in different location.

Source	NH <sub>4</sub> <sup>+</sup>	N + N	Location	Sampling Periods
[31]	20.6–19.6	12.6–8.6 *	PRD (Pearl River Delta) region	2010 to 2017
[19]	12.99	7.68	Jiao Zhou Bay, Yellow Sea	2015 to 2016
[40]	25.1	27.4 *	Guangzhou	2008
[33]	1.96–3.78	2.38–3.36	East Sea	March 2014 to February 2016

\*, Flux of only NO<sub>3</sub><sup>-</sup>; Unit: kg N·ha<sup>-1</sup>·a<sup>-1</sup>.

**Table 3.** Total wet N deposition.

Source	TN	Location
[36,37]	16.3–28.2	Northern China
[38]	26.8	Yangtze River Delta
[41]	27	Tai lake region
[31]	12.17–51.93	TGR (the Pearl River Delta) region
[43]	1.7–3.5	US
[44]	6.58	Europe

Unit: kg·N·ha<sup>-1</sup>·a<sup>-1</sup>.

The inland areas were less affected by long-distance ocean air masses, and the meteorological conditions were not as conducive to the diffusion of pollutants. Compared with coastal areas, inland areas have less precipitation, so dry deposition was the leading deposition vehicle. For these reasons, the atmospheric nitrogen deposition was significantly higher in inland than coastal areas. This delta region has been greatly affected by human urbanization related activities, such as artificial fertilization and coal burning, and as such has high N deposition, most of which is NH<sub>4</sub><sup>+</sup>. Excess deposition of nitrogen and sulfur can lead to increased acidification of water and soil, especially in areas with low alkalinity or weak acid neutralization capacity (ANC), such as at high altitudes [46–48]. By analyzing the data and establishing a model, it has been shown that the precipitation time interval also has an important influence on wet deposition [8].

#### 4. Conclusions

Wet deposition samples from an urban coastal region in China were analyzed using ion chromatography and shown to contain nine dissolved ions of which SO<sub>4</sub><sup>2-</sup>, NO<sub>3</sub><sup>-</sup>, Cl<sup>-</sup>, and NH<sub>4</sub><sup>+</sup> comprised over 80% of the average sample mass. Using HYSPLIT to simulate backward trajectories of air masses which impact the Xiamen region, combined with PMF and PCA analyses, three source terms were identified that impact the composition of wet deposition at the sample site: agricultural N fertilization and biomass burning, secondary aerosol formation, and aerosols of marine origin. The deposition of NO<sub>3</sub><sup>-</sup>

N peaked at  $507.5 \text{ mg}\cdot\text{N}\cdot\text{m}^{-2}\cdot\text{month}^{-1}$  in May and  $\text{NH}_4^+\text{-N}$  deposition peaked at  $99.8 \text{ mg}\cdot\text{N}\cdot\text{m}^{-2}\cdot\text{month}^{-1}$  in June. The highest concentration of  $\text{NO}_3^-$  was in the month of May at a value of  $75 \text{ mg/L}$ , while the concentration of  $\text{NH}_4^+$  varied from  $1.2$  to  $16 \text{ mg/L}$  overall. The highest concentrations for both ions were in the spring and lowest during the summer months. Total N deposition during the rainy season (5 months) was  $11 \text{ kg}\cdot\text{N}\cdot\text{ha}^{-1}$ .

In this paper, we summarize the composition of wet deposition received at a coastal urban area (Xiamen, China) during the rainy season in 2014. Subsequent calculation of nutrient fluxes identified  $\text{NO}_3^-$  as the dominant source of N in wet deposition. This suggests that control of vehicle numbers and exhaust emissions could have a positive impact on reducing N-loading to this area in the future. This study adds to the limited database regarding nitrogen deposition in coastal cities. Despite having relatively few samples and a short period, this study can be used as a reference for populated coastal cities, and it would contribute to the development of strategies for eutrophication of local water bodies and environment, as well as to examining the influence of N deposition as a nutrient source on primary productivity in the biosphere.

**Author Contributions:** Conceptualization, H.Y., J.S., M.Z. and L.J.; Data curation, Q.L., Y.L. and S.X.; Writing—original draft, Y.F.; Writing—review & editing, S.Z., S.W. and J.Y. All authors have read and agreed to the published version of the manuscript.

**Funding:** This research was funded by the Scientific Research Foundation of Third Institute of Oceanography, MNR. (no. 2020015), Qingdao National Laboratory for Marine Science and Technology (no. QNLM2016ORP0109), the Natural Science Foundation of Fujian Province, China (no. 2019J01120).

**Institutional Review Board Statement:** Not applicable.

**Informed Consent Statement:** Not applicable.

**Data Availability Statement:** <https://zenodo.org/record/5629882>, accessed on 10 September 2021.

**Acknowledgments:** This study is financially supported by the Scientific Research Foundation of Third Institute of Oceanography, MNR. (no. 2020015), Qingdao National Laboratory for Marine Science and Technology (no. QNLM2016ORP0109), the Natural Science Foundation of Fujian Province, China (no. 2019J01120).

**Conflicts of Interest:** The authors declare no conflict of interest.

## References

1. Ti, C.; Xia, Y.; Pan, J.; Gu, G.; Yan, X. Nitrogen budget and surface water nitrogen load in Changshu: A case study in the Taihu Lake region of China. *Nutr. Cycl. Agroecosyst.* **2011**, *91*, 55. [[CrossRef](#)]
2. Johansen, A.M.; Duncan, C.; Reddy, A.; Swain, N.; Sorey, M.; Nieber, A.; Agren, J.; Lenington, M.; Bolstad, D.; Samora, B.; et al. Precipitation chemistry and deposition at a high-elevation site in the Pacific Northwest United States (1989–2015). *Atmos. Environ.* **2019**, *212*, 221–230. [[CrossRef](#)]
3. Streets, D.G.; Bond, T.C.; Carmichael, G.R.; Fernandes, S.D.; Fu, Q.; He, D.; Klimont, Z.; Nelson, S.M.; Tsai, N.Y.; Wang, M.Q.; et al. An inventory of gaseous and primary aerosol emissions in Asia in the year 2000. *J. Geophys. Res. Atmos.* **2003**, *108*. [[CrossRef](#)]
4. Yu, W.T.; Jiang, C.M.; Ma, Q.; Xu, Y.G.; Zou, H.; Zhang, S.C. Observation of the nitrogen deposition in the lower Liaohe River Plain, Northeast China and assessing its ecological risk. *Atmos. Res.* **2011**, *101*, 460–468. [[CrossRef](#)]
5. Russell, K.M.; Galloway, J.N.; Macko, S.A.; Moody, J.L.; Scudlark, J.R. Sources of nitrogen in wet deposition to the Chesapeake Bay region. *Atmos. Environ.* **1998**, *32*, 2453–2465. [[CrossRef](#)]
6. Fenn, M.E.; Bytnerowicz, A.; Schilling, S.L.; Vallano, D.M.; Zavaleta, E.S.; Weiss, S.B.; Morozumi, C.; Geiser, L.H.; Hanks, K. On-road emissions of ammonia: An underappreciated source of atmospheric nitrogen deposition. *Sci. Total Environ.* **2018**, *625*, 909–919. [[CrossRef](#)]
7. Decina, S.M.; Hutyrá, L.R.; Templer, P.H. Hotspots of nitrogen deposition in the world's urban areas: A global data synthesis. *Front. Ecol. Environ.* **2020**, *18*, 92–100. [[CrossRef](#)]
8. Peretti, M.; Piñeiro, G.; Fernández Long, M.E.; Canelos, D.A. Influence of the precipitation interval on wet atmospheric deposition. *Atmos. Environ.* **2020**, *237*, 117580. [[CrossRef](#)]
9. Huang, P.; Zhang, J.; Zhu, A.; Xin, X.; Zhang, C.; Ma, D. Atmospheric deposition as an important nitrogen load to a typical agroecosystem in the Huang-Huai-Hai Plain. 1. Measurement and preliminary results. *Atmos. Environ.* **2011**, *45*, 3400–3405. [[CrossRef](#)]

10. Xu, W.; Wen, Z.; Shang, B.; Dore, A.J.; Tang, A.; Xia, X.; Zheng, A.; Han, M.; Zhang, L.; Zhao, Y.; et al. Precipitation chemistry and atmospheric nitrogen deposition at a rural site in Beijing, China. *Atmos. Environ.* **2020**, *223*, 117253. [[CrossRef](#)]
11. Huang, Z.; Wang, S.; Zheng, J.; Yuan, Z.; Ye, S.; Kang, D. Modeling inorganic nitrogen deposition in Guangdong province, China. *Atmos. Environ.* **2015**, *109*, 147–160. [[CrossRef](#)]
12. Shen, J.; Li, Y.; Liu, X.; Luo, X.; Tang, H.; Zhang, Y.; Wu, J. Atmospheric dry and wet nitrogen deposition on three contrasting land use types of an agricultural catchment in subtropical central China. *Atmos. Environ.* **2013**, *67*, 415–424. [[CrossRef](#)]
13. Lu, C.; Tian, H. Half-century nitrogen deposition increase across China: A gridded time-series data set for regional environmental assessments. *Atmos. Environ.* **2014**, *97*, 68–74. [[CrossRef](#)]
14. Wu, S.-P.; Zhang, Y.-J.; Schwab, J.J.; Li, Y.-F.; Liu, Y.-L.; Yuan, C.-S. High-resolution ammonia emissions inventories in Fujian, China, 2009–2015. *Atmos. Environ.* **2017**, *162*, 100–114. [[CrossRef](#)]
15. Wu, S.P.; Zhu, H.; Liu, Z.; Dai, L.H.; Zhang, N.; Schwab, J.J.; Yuan, C.S.; Yan, J.P. Nitrogen isotope composition of ammonium in PM(2.5) in the Xiamen, China: Impact of non-agricultural ammonia. *Environ. Sci. Pollut. Res. Int.* **2019**, *26*, 25596–25608. [[CrossRef](#)]
16. Li, Y.; Cui, S.; Gao, B.; Tang, J.; Huang, W.; Huang, Y. Modeling nitrogen flow in a coastal city—A case study of Xiamen in 2015. *Sci. Total Environ.* **2020**, *735*, 139294. [[CrossRef](#)]
17. Zhang, Y.; Wu, S.-Y. Fine Scale Modeling of Agricultural Air Quality over the Southeastern United States Using Two Air Quality Models. Part II. Sensitivity Studies and Policy Implications. *Aerosol Air Qual. Res.* **2013**, *13*, 1475–1491. [[CrossRef](#)]
18. Backes, A.M.; Aulinger, A.; Bieser, J.; Matthias, V.; Quante, M. Ammonia emissions in Europe, part II: How ammonia emission abatement strategies affect secondary aerosols. *Atmos. Environ.* **2016**, *126*, 153–161. [[CrossRef](#)]
19. Fu, X.; Wang, S.; Xing, J.; Zhang, X.; Wang, T.; Hao, J. Increasing Ammonia Concentrations Reduce the Effectiveness of Particle Pollution Control Achieved via SO<sub>2</sub> and NO<sub>x</sub> Emissions Reduction in East China. *Environ. Sci. Technol. Lett.* **2017**, *4*, 221–227. [[CrossRef](#)]
20. Wang, S.; Yan, Y.; Yu, R.; Shen, H.; Hu, G.; Wang, S. Influence of pollution reduction interventions on atmospheric PM<sub>2.5</sub>: A case study from the 2017 Xiamen. *Atmos. Pollut. Res.* **2021**, *12*, 101137. [[CrossRef](#)]
21. Sun, L.; Zhang, X.; Zheng, J.; Zheng, Y.; Yuan, D.; Chen, W. Mercury concentration and isotopic composition on different atmospheric particles (PM<sub>10</sub> and PM<sub>2.5</sub>) in the subtropical coastal suburb of Xiamen Bay, Southern China. *Atmos. Environ.* **2021**, *261*, 118604. [[CrossRef](#)]
22. Zhao, S.; Chen, L.; Yan, J.; Chen, H. Characterization of lead-containing aerosol particles in Xiamen during and after Spring Festival by single-particle aerosol mass spectrometry. *Sci. Total Environ.* **2017**, *580*, 1257–1267. [[CrossRef](#)]
23. Zhao, S.; Chen, L.; Yan, J.; Shi, P.; Li, Y.; Li, W. Characteristics of Particulate Carbon in Precipitation during the Rainy Season in Xiamen Island, China. *Atmosphere* **2016**, *7*, 140. [[CrossRef](#)]
24. Norris, G.; Duvall, R.; Brown, S.; Bai, S. EPA Positive Matrix Factorization (PMF) 5.0 Fundamentals and User Guide. 2014. Available online: [https://www.epa.gov/sites/default/files/2015-02/documents/pmf\\_5.0\\_user\\_guide.pdf](https://www.epa.gov/sites/default/files/2015-02/documents/pmf_5.0_user_guide.pdf) (accessed on 10 September 2021).
25. Chang, D.; Wang, Z.; Guo, J.; Li, T.; Liang, Y.; Kang, L.; Xia, M.; Wang, Y.; Yu, C.; Yun, H.; et al. Characterization of organic aerosols and their precursors in southern China during a severe haze episode in January 2017. *Sci. Total Environ.* **2019**, *691*, 101–111. [[CrossRef](#)] [[PubMed](#)]
26. Wu, S.-P.; Dai, L.-H.; Wei, Y.; Zhu, H.; Zhang, Y.-J.; Schwab, J.J.; Yuan, C.-S. Atmospheric ammonia measurements along the coastal lines of Southeastern China: Implications for inorganic nitrogen deposition to coastal waters. *Atmos. Environ.* **2018**, *177*, 1–11. [[CrossRef](#)]
27. Duan, F.; Liu, X.; Yu, T.; Cachier, H. Identification and estimate of biomass burning contribution to the urban aerosol organic carbon concentrations in Beijing. *Atmos. Environ.* **2004**, *38*, 1275–1282. [[CrossRef](#)]
28. Roth, B.; Okada, K. On the modification of sea-salt particles in the coastal atmosphere. *Atmos. Environ.* **1998**, *32*, 1555–1569. [[CrossRef](#)]
29. AzadiAghdam, M.; Braun, R.A.; Edwards, E.-L.; Bañaga, P.A.; Cruz, M.T.; Betito, G.; Cambaliza, M.O.; Dadashazar, H.; Lorenzo, G.R.; Ma, L.; et al. On the nature of sea salt aerosol at a coastal megacity: Insights from Manila, Philippines in Southeast Asia. *Atmos. Environ.* **2019**, *216*. [[CrossRef](#)]
30. Zheng, L.; Chen, W.; Jia, S.; Wu, L.; Zhong, B.; Liao, W.; Chang, M.; Wang, W.; Wang, X. Temporal and spatial patterns of nitrogen wet deposition in different weather types in the Pearl River Delta (PRD), China. *Sci. Total Environ.* **2020**, *740*, 139936. [[CrossRef](#)]
31. Hara, H. Acid deposition chemistry in Asia, Europe, and North America. *Prog. Nucl. Energy* **1998**, *32*, 331–338. [[CrossRef](#)]
32. Fakhraei, H.; Driscoll, C.T.; Renfro, J.R.; Kulp, M.A.; Blett, T.F.; Brewer, P.F.; Schwartz, J.S. Critical loads and exceedances for nitrogen and sulfur atmospheric deposition in Great Smoky Mountains National Park, United States. *Ecosphere* **2016**, *7*, e01466. [[CrossRef](#)]
33. Heng, Z. Study on Pollution Characteristics and Sources of Ammonia and Atmospheric Nitrogen Deposition Flux in Xiamen Bay. Master's Thesis, Xiamen University, Xiamen, China, 2019. Available online: <https://oversea.cnki.net/KCMS/detail/detail.aspx?dbcode=CMFD&dbname=CMFD202002&filename=1019064510.nh&uniplatform=NZKPT&v=3x5tH%25mmd2BbNTR2yBo902x3N8tPhHuZHpbUMmWhUyr0aHgMwS%25mmd2BSNpUZ18cPajg7gdtj> (accessed on 10 September 2021).

34. Park, G.-H.; Lee, S.-E.; Kim, Y.-I.; Kim, D.; Lee, K.; Kang, J.; Kim, Y.-H.; Kim, H.; Park, S.; Kim, T.-W. Atmospheric deposition of anthropogenic inorganic nitrogen in airborne particles and precipitation in the East Sea in the northwestern Pacific Ocean. *Sci. Total Environ.* **2019**, *681*, 400–412. [[CrossRef](#)] [[PubMed](#)]
35. Leng, Q.; Cui, J.; Zhou, F.; Du, K.; Zhang, L.; Fu, C.; Liu, Y.; Wang, H.; Shi, G.; Gao, M.; et al. Wet-only deposition of atmospheric inorganic nitrogen and associated isotopic characteristics in a typical mountain area, southwestern China. *Sci. Total Environ.* **2018**, *616–617*, 55–63. [[CrossRef](#)]
36. Qi, J.H.; Shi, J.H.; Gao, H.W.; Sun, Z. Atmospheric dry and wet deposition of nitrogen species and its implication for primary productivity in coastal region of the Yellow Sea, China. *Atmos. Environ.* **2013**, *81*, 600–608. [[CrossRef](#)]
37. Zhang, Y.; Liu, X.J.; Fangmeier, A.; Goulding, K.T.W.; Zhang, F.S. Nitrogen inputs and isotopes in precipitation in the North China Plain. *Atmos. Environ.* **2008**, *42*, 1436–1448. [[CrossRef](#)]
38. Luo, X.S.; Liu, P.; Tang, A.H.; Liu, J.Y.; Zong, X.Y.; Zhang, Q.; Kou, C.L.; Zhang, L.J.; Fowler, D.; Fangmeier, A.; et al. An evaluation of atmospheric Nr pollution and deposition in North China after the Beijing Olympics. *Atmos. Environ.* **2013**, *74*, 209–216. [[CrossRef](#)]
39. Zhao, X.; Yan, X.; Xiong, Z.; Xie, Y.; Xing, G.; Shi, S.; Zhu, Z. Spatial and Temporal Variation of Inorganic Nitrogen Wet Deposition to the Yangtze River Delta Region, China. *Water Air Soil Pollut.* **2009**, *203*, 277–289. [[CrossRef](#)]
40. Jia, G.; Chen, F. Monthly variations in nitrogen isotopes of ammonium and nitrate in wet deposition at Guangzhou, south China. *Atmos. Environ.* **2010**, *44*, 2309–2315. [[CrossRef](#)]
41. Xie, Y.; Xiong, Z.; Xing, G.; Yan, X.; Shi, S.; Sun, G.; Zhu, Z. Source of nitrogen in wet deposition to a rice agroecosystem at Tai lake region. *Atmos. Environ.* **2008**, *42*, 5182–5192. [[CrossRef](#)]
42. Kuang, F.; Liu, X.; Zhu, B.; Shen, J.; Pan, Y.; Su, M.; Goulding, K. Wet and dry nitrogen deposition in the central Sichuan Basin of China. *Atmos. Environ.* **2016**, *143*, 39–50. [[CrossRef](#)]
43. Chang, C.-T.; Wang, C.-P.; Huang, J.-C.; Wang, L.-J.; Liu, C.-P.; Lin, T.-C. Trends of two decadal precipitation chemistry in a subtropical rainforest in East Asia. *Sci. Total Environ.* **2017**, *605–606*, 88–98. [[CrossRef](#)]
44. Du, E.; de Vries, W.; Galloway, J.N.; Hu, X.; Fang, J. Changes in wet nitrogen deposition in the United States between 1985 and 2012. *Environ. Res. Lett.* **2014**, *9*, 095004. [[CrossRef](#)]
45. Holland, E.A.; Braswell, B.H.; Sulzman, J.; Lamarque, J.-F. Nitrogen Deposition onto The United States and Western Europe: Synthesis of Observations and Models. *Ecol. Appl.* **2005**, *15*, 38–57. [[CrossRef](#)]
46. Fenn, M.E.; Bytnerowicz, A.; Liptzin, D. Nationwide Maps of Atmospheric Deposition Are Highly Skewed When Based Solely on Wet Deposition. *BioScience* **2012**, *62*, 621.
47. Greaver, T.L.; Sullivan, T.J.; Herrick, J.D.; Barber, M.C.; Baron, J.S.; Cosby, B.J.; Deerhake, M.E.; Dennis, R.L.; Dubois, J.-J.B.; Goodale, C.L.; et al. Ecological effects of nitrogen and sulfur air pollution in the US: What do we know? *Front. Ecol. Environ.* **2012**, *10*, 365–372. [[CrossRef](#)]
48. Vet, R.; Artz, R.S.; Carou, S.; Shaw, M.; Ro, C.-U.; Aas, W.; Baker, A.; Bowersox, V.C.; Dentener, F.; Galy-Lacaux, C.; et al. A global assessment of precipitation chemistry and deposition of sulfur, nitrogen, sea salt, base cations, organic acids, acidity and pH, and phosphorus. *Atmos. Environ.* **2014**, *93*, 3–100. [[CrossRef](#)]